Rapid phase shifting fiber interferometer with optical stylus

H. Martin and X. Jiang*

University of Huddersfield, Queensgate, Huddersfield HD1 3DH, UK

* *Corresponding author: x.jiang@hud.ac.uk*

ABSTRACT

Optical fiber interferometry holds many advantages for the online measurement of high precision surfaces. Here a fiber interferometer with a wavelength scanning probe is reported. Such an interferometer requires active stabilization against the effects of temperature drift and vibration. A method of multiplexing dual wavelengths into the same fiber, combined with rapid phase shifting and real time phase calculation is investigated. Experimental data show the successful stabilization of the interferometer regardless of environmental perturbation.

OCIS codes: *120.0120, 120.3180, 120.5050*.

Technological advances in fields such as optics, micro-molding and micro-machining have resulted in the increased use of nano-scale and ultra-precision surfaces. The current state of online surface metrology methods for the efficient characterization of these surfaces is severely limiting both development and manufacture. Current metrology instrumentation is either too bulky, slow or damaging (in the case of touch probe methods) [1].

Our approach is to use interferometry combined with single-point scanning, the idea being analogous to a traditional contact stylus for surface profile measurement, but realized in the optical domain. By combining the probe with one arm of an optical fiber interferometer it is possible place the bulk of the other optical components and electronics remotely. In this way a compact probe may be realized which is suitable for remote mounting.

The concept of an optical stylus provides the advantages of speed and non-contact measurement. By tuning the wavelength of the source light and using a dispersive element it is possible to diffract a beam of light over a desired angular range. An objective lens is then used to collimate the beam onto the surface to be measured. In this way the beam may be swept along a profile of the surface in the manner of a stylus, the retro-reflected light may then be analyzed by an interferometer to determine the phase variation which relates directly to surface height. The apparatus investigated in this paper, including the optical probe, is illustrated in fig. 1.

A tunable laser source (TLS), swept between an optical wavelength of $1560 \leq \lambda_m \leq 1575$ nm and provides the light source for enabling the optical stylus technique. The profile length and lateral resolution available is dependant on the objective lens and grating parameters which are selectable depending on the application. The wavelength is swept during measurement to interrogate the surface profile.

Unfortunately the use of optical fibers for nanometer scale surface measurement brings a specific set of challenges. It is well documented that fiber interferometers are extremely sensitive to environmental perturbation [2]. Temperature variations and vibration cause deformation and stresses in the fiber core which changes the optical path length. The magnitude of the path length change scales linearly with the length of fiber; with the approximately 20 meters of fiber used in this experimental setup, temperature drift alone can result in several microns of path change, completely obliterating any measurement at the nanometric scale.

The same mechanisms also cause random evolution of the state of polarization (SOP) of the light carried in the fiber. Generally, a length of fiber may be modeled as an elliptical birefringence having random, time varying axis of orientation and rotational magnitude [3]. SOP variations have two primary effects on the output of an interferometer. First, the fringe visibility (or contrast) is dependant on the relative SOP in each interferometer arm as well as the SOP in the input fiber [4]. Second, any polarization dependence of components within the optical circuits results in intensity fluctuation. In our experimental set up described there are two main contributors; the blazed diffraction grating and the electro-optic phase modulator (EOPM), which has an integrated linear polariser.

The time varying quantities due to both the optical path length and SOP fluctuation may be incorporated into the basic interferometer response equation. Here, the intensity response, $I(t)$ of an interferometer is given by

$$I(t) = I_{ref}(t) + I_{sen}(t) + V(t)\sqrt{I_{ref}(t) I_{sen}(t)} \cdot \cos\left[\varphi + \varepsilon(t)\right] \quad (1)$$

where $I_{ref}(t)$, $I_{sen}(t)$ are the light intensities from the reference and sense arms respectively, the time dependence describes intensity fluctuation due to SOP change. $\varphi = 4\pi h / \lambda$ is the phase difference resulting from the variation in surface height, h for a given source light wavelength, λ. $\varepsilon(t)$ is an error term describing the time varying phase difference induced by fiber path length drifting. $V(t)$ is the fringe visibility term (between zero and unity), the value of which varies with SOP evolution. The equation assumes balanced operation of the interferometer i.e. the optical path lengths in each arm are equal.

In order to track the optical path length change, a separate reference wavelength is multiplexed into the fiber interferometer. This is sourced by a narrowband distributed feedback laser diode operating at a wavelength, $\lambda_r = 1550\text{ nm}$. As the wavelength remains static while the optical stylus is swept over the surface, it remains fixed upon one point of the surface. This static reference interferometer (as it shall now be referred to) shares a near-common path with the measurement interferometer. It may thus be used to track the unwanted phase disturbance caused by path length drift in the fiber as well as any vibration of the measurand (along the measurement axis).

The feedback from the reference interferometer is used in a servo loop, with a path length actuator in the reference arm, to simultaneously stabilize both the phase change occurring due to the fiber and vibration of the measurand. An electro-optic phase modulator (EOPM) is employed as the path length actuator. The EOPM provides a high frequency response (>1 GHz) and very good linearity.

It is clear from equation 1 that the output intensity is not purely a function of phase, thus in order to calculate track the error term, $\varepsilon(t)$ the phase of the interferometer must be derived directly.

The method employed is to use a digital signal processor (DSP) in order to calculate the reference interferometer phase in realtime. This is done by shifting the phase of the interferometer stepwise and then sampling the resulting intensity values. The method is a variation on common phase shifting interferometry, however in this case it is carried out very quickly by virtue of the EOPM response [5]. In essence the EOPM allows the possibility of deriving phase in realtime.

The Schwider-Hariharan 5-step phase shifting algorithm is executed on the DSP to calculate the phase value [6]. The algorithm was chosen because it is reasonably efficient in calculation assuming a phase shift of π/2 is adopted. Using this algorithm the phase is calculated as,

$$\varphi = \tan^{-1}\frac{2(I_2 - I_4)}{I_1 - 2I_3 + I_5} \tag{2}$$

where I_1, I_2, I_3, I_4 and I_5 are the intensities at phase shifts of 0, π/2, π, 3 π/4 and 2π radians respectively.

The principle relies on the fact that SOP and optical path length drift occur at low frequencies (<1 kHz). By carrying out phase shifting at a much higher frequency, the intensity error imposed by SOP and optical path length drift are negligible between shifts. In this way a stable and accurate phase result may be retrieved even in the face of low frequency intensity variations.

The realtime calculated phase values are used as the feedback element to a digital proportional-integral (PI) controller. The controller then adjusts an offset voltage on the EOPM output in order to keep the calculated phase value stable. In this way the EOPM provides both the phase stepping required to retrieve the phase and also operates on the optical path length to keep the interferometer stable. The overall execution time for the phase calculation and control algorithm is approximately 27 μs, yielding an overall control loop rate of 37 kHz.

Fig. 2 shows the output of the reference interferometer sampled at 100 Hz over a 2 second period. The drift experienced in the free running mode is substantial and covers several hundred nanometers, even though the apparatus was mounted on a vibration isolated optical table. The improvement seen when the feedback loop is activated is substantial.

In order to gain a more quantitative analysis of the stabilized interferometer performance, the output of the measurement interferometer was sampled. Fig. 3 shows the collected measurement interferometer data for a period of 10 seconds at a sample rate of 100 Hz. The data was collected at 4 different wavelengths, which correspond to four different points along the profile of the surface. This was done to check there was a consistent level over stabilization over the full scan profile. The target surface was a low quality mirror having 4λ/inch surface deviation, so the obtained height information was somewhat arbitrary. Since aim of this experiment was to compare the stability across the profile, the results were all centered about their means to simplify comparison. The peak-to-peak variation is seen to be ± 11nm and the overall noise level does not appear to change significantly along the scanned profile.

Fig. 4(a) shows the profile measurement of a step height sample as taken with a Taylor Hobson CCI 6000 white light interferometer. Fig 4(b) shows the profile of the step height in approximately the same area using our fiber interferometer. The calculated heights and overall profile show good correlation, although there is clearly a higher level of noise present on the fiber interferometer output however. This step is not resolved as sharply with the fiber interferometer, this is anticipated to be because of currently non-optimized optics. For this reason a longer sampling period is apparent in fig. 4(b) as lowering it did not improve the lateral resolution.

The overall noise magnitudes were found to be consistent with the quantization noise that might be expected to occur from the 12 bit analog to digital converter used to sample the intensity values. It is anticipated that by swapping this device for a higher resolution ADC the noise results may be improved substantially.

To conclude, a fiber interferometer, designed for surface metrology applications and featuring a non-contact optical stylus, was built and investigated. In order for such an apparatus to be feasible for nanoscale measurement the optical path lengths of the fiber must be stabilized against temperature drifts and mechanical disturbance. A rapid phase shifting technique utilizing wavelength multiplexed interferometers was employed in order to do this effectively. The stability is currently limited by the quantization noise imparted by the analog to digital converter used.

Acknowledgements

The corresponding author X. Jiang gratefully acknowledges the Royal Society under a Wolfson-Royal Society Research Merit Award and the European Research Council under its program ERC-2008-AdG 228117-Surfund.

References

1. L. Singleton, R. Leach, A. Lewis and Z. Cui, Report on the analysis of the MEMSTAND survey on Standardisation of MicroSystems Technology, MEMSTAND Project IST-2001-37682 (2002).
2. D. Jackson, R. Priest, A. Dandridge and A. Tveten, Appl. Opt. 19(17), 2926-2929 (1980).
3. I. Kaminow, Journal of Quantum Electronics. 17(1), 15-22 (1981).
4. A. Kersey, M. Marrone and A. Dandridge, J. Lightwave Tech. 8(6), 838-845 (1990).
5. K. Creath, Phase-Measurement Interferometry Techniques. In E. Wolf (ed.) Progress in Optics. XXVI. (Amsterdam, Elsevier Science Publishers, 1998).
6. J. Schwider, R. Burow, K. Elssner, J. Grzanna, R. Spolaczyk and K. Merkel, Appl. Opt., 22(21), 3421-3432 (1983).

Fig. 1 Experimental Apparatus

Fig. 2 Drift seen in the stabilized/free running reference interferometer

Fig. 3 Histograms of stabilized measurement interferometer values

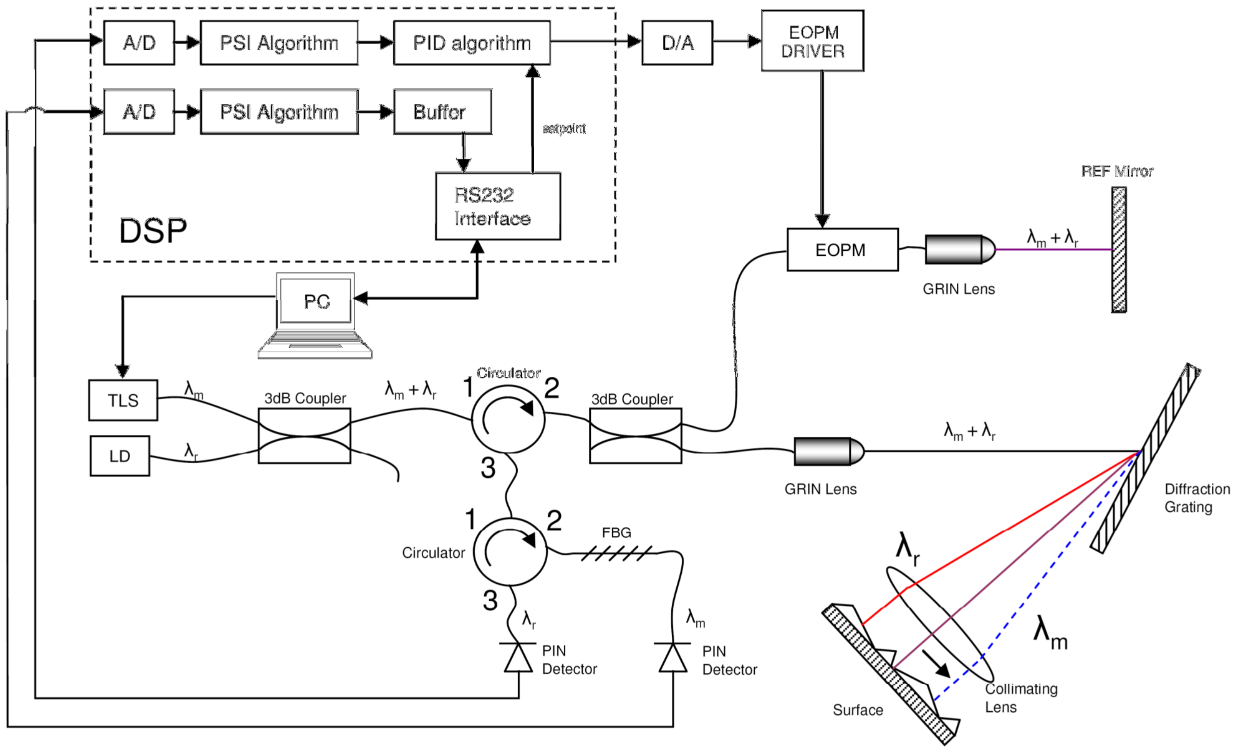

Fig. 1 Experimental Apparatus

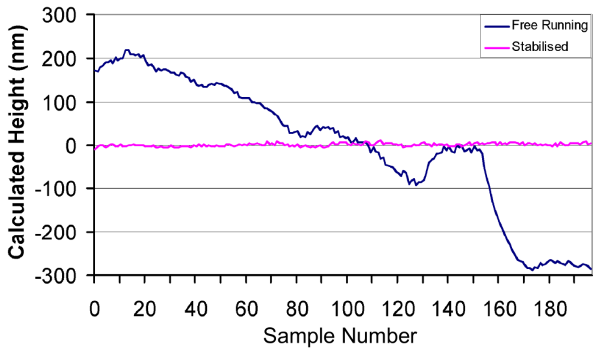

Fig. 2 Drift seen in the reference interferometer

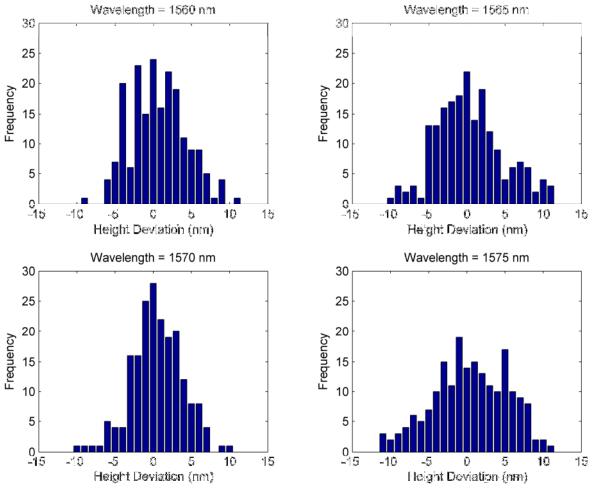

Fig. 3 Histograms of stabilized measurement interferometer values

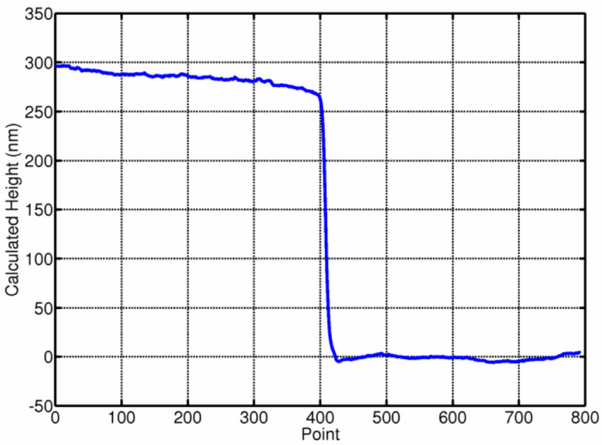

(a)

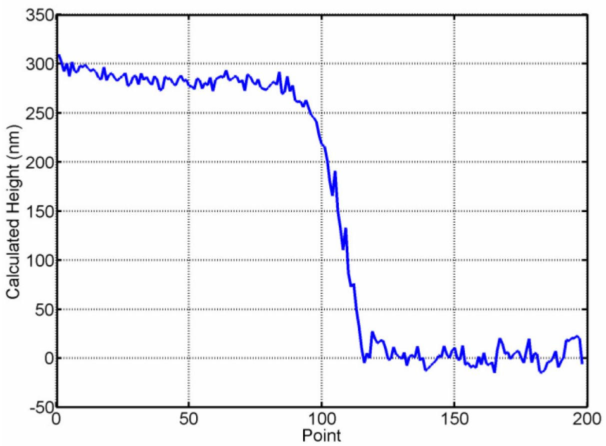

(b)

Fig. 4 Profile measurement of a step height from (a) Taylor Hobson CCI (b) Multiplexed Fiber Interferometer